

Protokoll
Neurobiologisches Großpraktikum

Response to communication signals of an off-type pyramidal cell in the ELL in *Apterous leptorhynchus*

Kathrin Root, Alexander Wendt, Patrick Weygoldt

Supervised by:

Jan Grewe & Alexandra Rudnaya
Neuroethology Group
Institute of Neurobiology
University of Tuebingen

February 13, 2023

1 Introduction

In the animal kingdom, different ways to communicate were invented in various species. Humans use spoken language to communicate with each other. This ability to use spoken language sets human primates apart from nonhuman primates (Ackermann et al., 2014). The production of this spoken language relies on muscle fibers and on the neural control mechanisms steering this complex action system with a high spatial and temporal accuracy (Ackermann et al., 2014). Animals like bats, rats and other rodents use ultrasonic vocalizations in their social interactions to communicate (Kanwal, 2018; Seffer et al., 2014). Another type of communication is used by insects like the southern green stink bug (*Nezara viridula* (L.)). Those insects use the mechanisms of vibrational communication through plants to transmit information about the species and sex of the sender and to provide directional cues for locating the mate (Virant-Doberlet et al., 2004).

Some aquatic animals like the electric eel, sharks or rays developed communication using electric signals (Catania, 2015; Kalmijn, 1971). This production of the electric signal is not only used in communication but also in navigation and prey capture (Hupé et al., 2008). For our project, we investigated the communication of the weakly electric fish *Apteronotus leptorhynchus*, which generates a weak electric field for communication and navigation (Harold Zakon et al., 2002). Electrocytes that are stretched over the whole body of the fish make up the electric organ which produces the electric organ discharge (EOD) that forms the electrocommunication signals (Hupé et al., 2008). The weakly electric fish also detects surrounding electric fields with sensory receptor cells called electroreceptors (Harold Zakon et al., 2002). This detection is not only used for surrounding electric fields but also for recognizing nearby objects by the distortions made in their electric field (Harold Zakon et al., 2002). This process is called electrolocation (Harold Zakon et al., 2002). *Apteronotus leptorhynchus* emits a continuous quasi-sinusoidal wave with a sexually dimorphic frequency (Hupé et al., 2008). Males have a frequency of 800–1000 Hz and females emit a frequency of 600–800 Hz (Harold Zakon et al., 2002). They are able to modulate their EOD frequency (EOD f) for social signaling (Harold Zakon et al., 2002). Possible types of EOD f modulations are the jamming avoidance response and social signals like chirps and rises (Raab et al., 2021; Harold Zakon et al., 2002). Interesting for our project are chirps which are social signal characterised by a transient increase in the EOD f . There are 4 types of chirps that are primarily used by males (Harold Zakon et al., 2002). Type 1 is a chirp with short duration lasting around 20 ms and with large frequency excursions of 200–300 Hz (Harold Zakon et al., 2002). Type 2 chirps also have a short duration around 20 ms but have a small frequency excursion of 50 Hz (Harold Zakon et al., 2002). Type 3 and 4 are chirps with a long duration 'lasting many to a few hundreds of milliseconds' (Harold Zakon et al., 2002) with a similar frequency excursion as type 1 chirps (Engler et al., 2000). While type 1 and type 2 are typically used in agonistic contexts, type 3 and type 4 are used for interacting and courting females (Harold Zakon et al., 2002). When two fish are near each other, 'their electric fields superimpose and add up at every point in space' (Walz et al., 2013). Each fish then perceives the merged signal, the so-called beat (Figure 1), which consists of the difference of the individual EOD f (Walz et al., 2013). Hagedorn et al., 1985 found that the EOD f is correlated with size and aggressiveness. This suggests that the beat frequency supplies information about the relative size and the aggressiveness of conspecifics (Walz et al., 2013) but this is still unclear and needs further investigation.

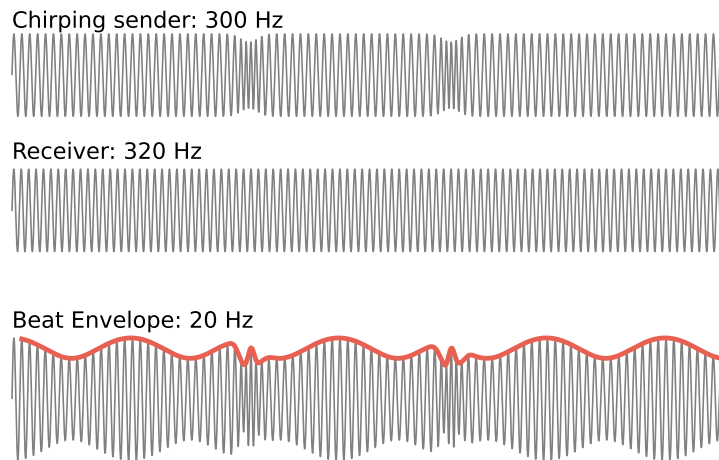


Figure 1 | Example of a beat with two chirps. Each chirp produces a transient change in the envelope, introducing a phase shift that differs, depending on the phase the chirp occurs in.

1.1 Neural pathways of electrocommunication

Important for us was, how electrocommunication is represented in the brain. The EOD is produced by the electric organ, which consists of several electroreceptor cells and is innervated by afferents that make up the octavolateralis nerve (H. Zakon, 1986). In this octavolateralis nerve are so-called P-units which have an irregular per-cycle firing rate that depends on the intensity of the amplitude received at the surface of the skin (Nelson et al., 1997). Those P-units project to different targets in the electrosensory lateral line lobe (ELL) of the hindbrain (Heiligenberg et al., 1982). The ELL is made up of the regions centromedial segment (CMS), centrolateral segment (CLS), lateral segment (LS) and medial segment (MS) (Carr et al., 1982). In the ELL the P-units trifurcate and project to the pyramidal neurons in the CMS, CLS, and LS (Carr et al., 1982). Pyramidal neurons in the ELL can be discriminated into superficial, intermediate and deep pyramidal cells based on different morphology and physiology (Figure 2, Bastian et al., 1991), which then project to the nucleus praeminentialis (nP) and the torus semicircularis (TS) (Rose, 2004). Those pyramidal cells can be distinguished into two types, the ON-cell (E-units) and the OFF-cell (I-units). While On-cells are excited by an increase in the EOD amplitude and receive their input from P-units, the OFF-cells are excited by a decrease in the EOD amplitude and also receive their input from P-units via interneurons (Berman et al., 1998).

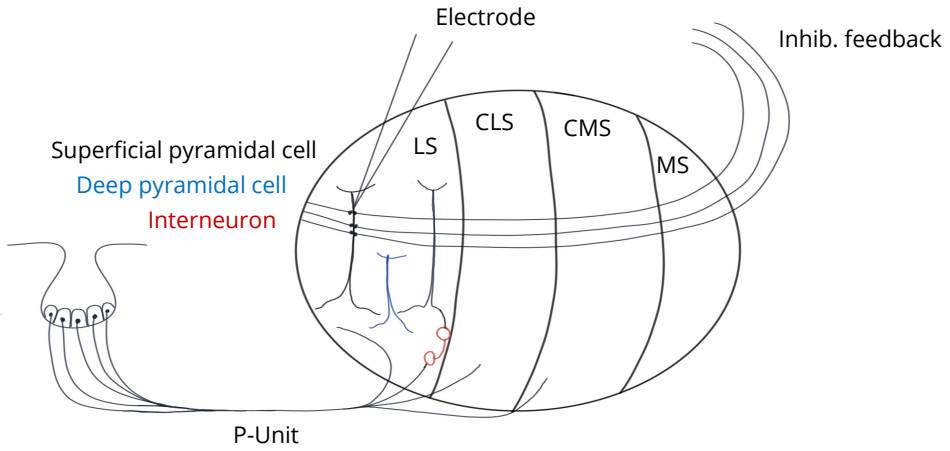


Figure 2 | Schematic of the neural pathways.

Pyramidal cells in the LS were found to be most important for the communication behavior because they fire preferably for beat frequencies above 8 Hz (W. Metzner et al., 1997). In addition lesions of the LS impair the response to chirps (Metzner et al., 1997). The ON-cells in the LS begin to burst if there is a frequency and phase shift in the beat frequency, indicating chirps (Marsat et al., 2009). On the other hand, OFF-cells can also detect chirps, but because they filter the signal with a low-pass filter, the response to a short but high-frequency excursion is poor (Marsat et al., 2009).

The aim of our project was to record pyramidal cells in the ELL in *Apterodonotus leptorhynchus*. We chose the LS region of the ELL because there the neurons are more likely to respond to our stimulus of a simulated chirping conspecific (W. Metzner et al., 1997). We wanted to identify the response properties of these cells with several well-known methods to identify the type of the recorded pyramidal cell. Furthermore, we wanted to compare how well the stimulus reconstruction is of pyramidal cells for bursting and single spikes.

2 Methods

2.1 Experimental animals

We used five *Apteronotus leptorhynchus* as subjects that were obtained from a tropical fish supplier (Aquarium Glaser GmbH, Rodnau, Germany) and kept in single tanks. The body sizes of the fish ranged from 14,5 cm - 17 cm and the weight ranged from 7,3 g - 14,9 g. Age and sex were unknown. The animals were kept in tanks with a water temperature of 25 °C and a conductivity of around 300 µS/cm in a light-dark cycle of 12 hours.

2.2 Surgery

All fish were anesthetized in MS222 solution with a concentration of 150 mg/L buffered in Sodium Bicarbonate (same concentration) until gill movement stopped, indicating the third stage of anaesthesia. Fish were then quickly weighed and measured before being transferred onto the surgery setup. During surgery, the gills were ventilated by administering a light flow of aerated and heated water via a tube inserted into the fish's mouth. The ventilation solution also contained a lighter dose (125 mg/L) of MS222 to keep the fish in anaesthesia. Excluding the areas that had to be opened, the full body of the fish was covered with damp paper towels to prevent the mucus membranes from drying out. Analgesia was provided by topically applied Lidocaine (2%) prior to opening the skin. Lidocaine application was then repeated to these areas every 1.5 hours. To fix the fish to the device for surgery and subsequent recording, we opened a small centered window on the dorsal side of the head between the eyes and the larger window marked for recording. Here, we dried the skull and attached a metal rod using Cyanacrylate. The main opening was always placed left to the center of the head shortly before the skull ends and the spinal cord begins. Before removing the skull, we assured the correct position using the blood vessels (t_0) visible through the translucent cranium. A reference electrode was inserted into a small cut in the skin. To immobilize the fish, a total of 50 µL Tubocurarine was injected into the muscles on either side.

2.3 Experimental setup

The surgery stage including the attached fish was then transferred into the experimental setup. The fish were submerged in water except for the opening in the skull. Borosilicate electrodes (1.5 m; GB150F-8P, Science Products, Hofheim, Germany) were pulled to a resistance of 50 MΩ (model P-97, Sutter Instruments, Novato, CA) and filled with 1 mol KCl solution. The silver wire was chlorinated in the morning of every recording day. Electrodes were lowered into the ELL using a microdrive (Luigs-Neumann, Ratingen, Germany). Recordings of the pyramidal cells were amplified (SEC-05, npi electronics, Tamm, Germany) and digitized at 40 kHz (PCI-6229, National Instruments, Austin, TX). RELACS (www.relacs.net) on a computer running Linux was used for EOD and online spike detection and recording as well as stimulus generation and calibration. If the fish started to show steep drops in EOD amplitude, we stopped the experiment and euthanized the subjects with MS222 (250 mg/L, 10 min) followed by decapitation.

2.4 Stimulation

The stimulus of a conspecific was projected by two horizontal electrodes (ISO-02V, npi-electronics, Tamm, Germany), that were placed 15 cm parallel to the fish. Chirps were produced by Gaussian frequency and amplitude modulations of the simulated fish. The phases of the beat in which the chirp occurred were random and not considered in the analysis. The simulated EOD range was between 10 Hz to 3300 Hz. For the F-I curve (Figure 10) we used a contrast range between -30 % to 30 %, whereas the

contrast displays the percentage change in the stimulus amplitude of the fish EOD. For each contrast, we used 10 trials. The STA (Figures 11 to 13), was calculated from a random amplitude modulation (RAM) that was displayed for 3,82 min.

2.5 Data analysis

We conducted all analyses using Python 3.10 and the libraries numpy, scipy, matplotlib, pandas, nixio and thunderfish (Adrian et al., 2014; Harris et al., 2020; Hunter, 2007; team, 2020; Virtanen et al., 2020). All time-dependent firing rates were estimated by convolving a gamma kernel (width = 2 ms) with the spike raster. Baseline firing rates were estimated by dividing the number of spikes detected by the duration of the baseline recording. To compute the beat of the signal measured in the recording setup, we computed the peaks of the beat in regions defined by the zero crossings of the signal (stimulus or fish) with the lower frequency. To obtain zero crossings, we rectified the signal. The resulting envelope was additionally interpolated (cubic) to obtain the same sampling interval as the recorded data. All spikes that are connected by an interspike interval that was lower than a 10 ms threshold were grouped and treated as a single temporal event at the time of the first spike in the respective burst. This threshold was the same as in Marsat et al., 2009. The spike triggered average stimulus was computed by extraction and averaging of the stimulus around - 40 ms and + 15 ms around every spike. To reconstruct the stimulus based on the spike triggered average, we used the spike triggered average as a kernel and convolved it with the original spike rasters. The reconstruction performance was quantified by the euclidean distance between the reconstruction and the stimulus (equation 1).

$$d(u, v) = \sqrt{\sum_{k=0}^n |u_k - v_k|^2} \quad (1)$$

3 Results

3.1 Characterizing the cell type

For the cell-type characterization we first recorded the baseline activity of each cell we found. With this recording of our principal cell, we detected 128 spikes in the presented time window (10 s). The baseline firing rate was at 12.8 Hz for this time window (Figure 3).

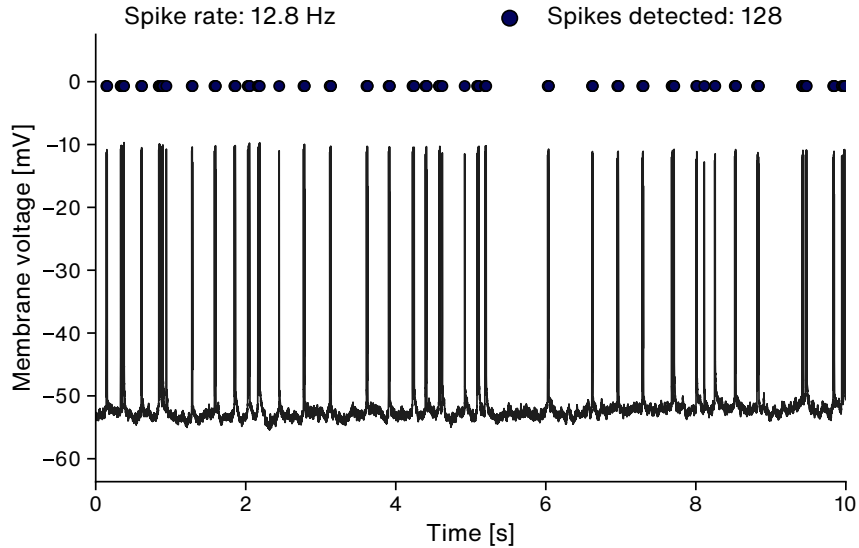


Figure 3 | Baseline activity of the recorded cell. Black dots are the detected spikes.

After recording the baseline, we stimulated the fish with chirps to see if the cell is reacting to the stimulus. When all different beat phases and frequencies of our stimulus were pooled together, the recorded cell did not show a response to the chirps (Figure 4). We did a comparison to an ON-cell recorded in the previous year, to get a clear picture of how it should look when a cell is responding to a chirp stimulus. Figure 4 shows this comparison for which we calculated a mean firing rate around the occurrence of a chirp. The mean firing rate was pooled over all trials that we recorded, and for that, we placed all chirp occurrences at the same time. The time in figure 4 is centered around a stimulation, i.e. around the playback of a chirp. For our cell (Figure 4 left) we can see that there is no response to the chirp at time zero. The firing rate (black line) does not change at any time. In contrast, the right sub-figure shows an apparent response to the occurrence of a chirp, which appears as an increase in the firing rate after time zero. For the case that the cell only coded for a chirp in a certain difference frequency, we also plotted the response pooled over all chirp stimuli separated by difference frequency (see figure 5 and figure 6).

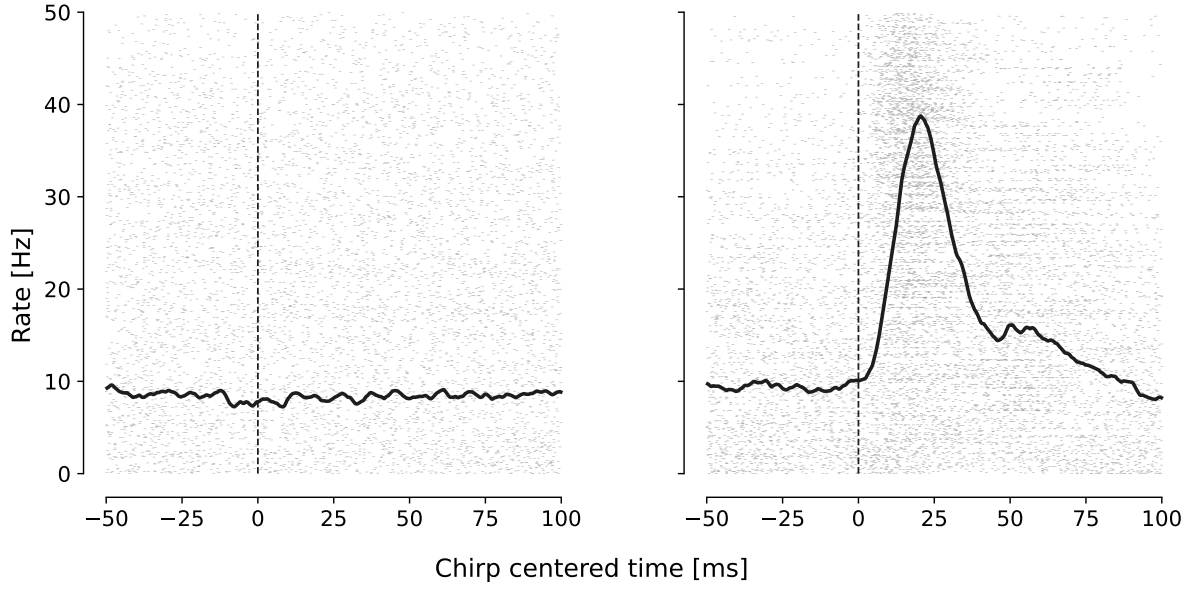


Figure 4 | Chirp triggered average spikes for the cell we recorded from (left) compared to a cell from previous recordings (right). Time is centered at the onset of a chirp. The line represents the instantaneous firing rate triggered by a chirp estimated by the convolution of a gamma kernel. This plot includes all chirp stimuli regardless of the phase of the chirp on the beat or the different frequencies used for stimulation.

For the relative EOD f of 1.05 Hz with a beat frequency of 30 Hz we found that this cell responds by reducing the spike rate after the chirp. The cell shows that it can have an off-response to the chirp stimulus, but this response is only observable with these stimulus parameters. (Figure 5).

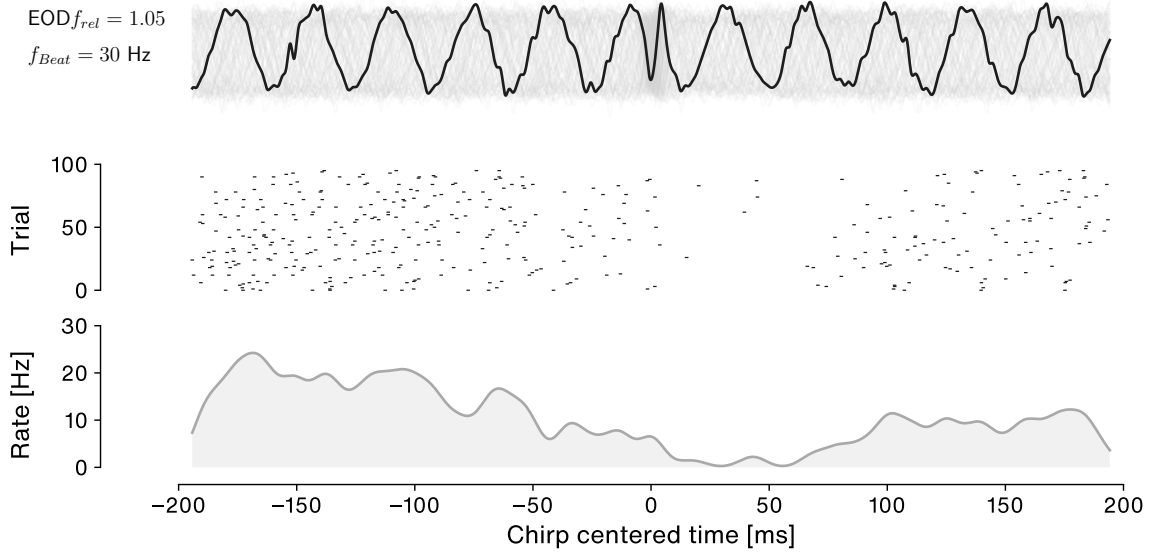


Figure 5 | Chirp triggered average with a relative EOD f of 1.05. Time is centered around the chirp. **Top:** stimulus signal with a relative EOD f of 1.05. The beat frequency was at 30 Hz. In black is one example trace of the stimulus. **Middle:** the Spike raster plot of the cell with 96 trials. **Bottom:** spike rate estimated with a gamma kernel.

With different multiples of EOD f , the responses do not change, and in all except for the previous example, the firing rate remains constant around a chirp (Figure 6). After this realization, we wanted to investigate the response to a stimulus without a chirp, and especially focus on if the cell might be phase-locked to

the beat.

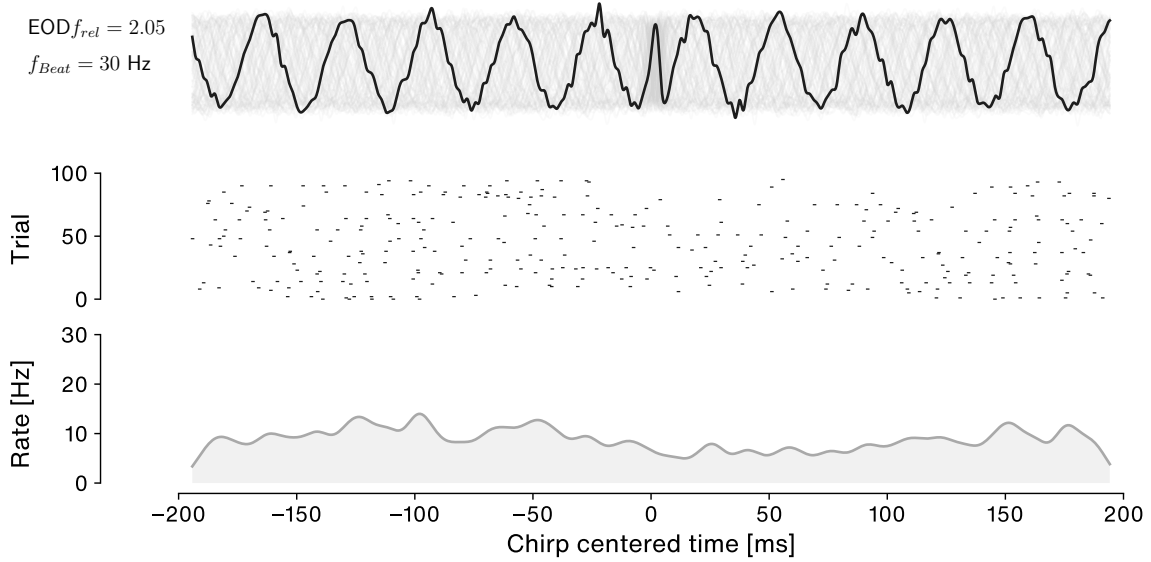


Figure 6 | Chirp triggered average with a relative $EODf$ of 2.05. Time is centered around the chirp. **Top:** stimulus signal with a relative $EODf$ of 2.05. The beat frequency was at 25 Hz. In black is one example trace of the stimulus. **Middle:** the spike raster plot of the cell with 96 trials. **Bottom:** spike rate estimated with a gamma kernel.

After combining the recordings in which we stimulated the fish with only a beat and grouping them only by phase, we found that the cells firing is phase-locked to certain beat frequencies (Figure 7). The cell increases the firing rate at times when the stimulus has a negative slope. This behavior is consistent with higher relative $EODf$ and higher beat frequencies (Figures 7 to 9). What we observed with these higher beat frequencies is that the response was weaker with higher frequencies and shifted its phase.

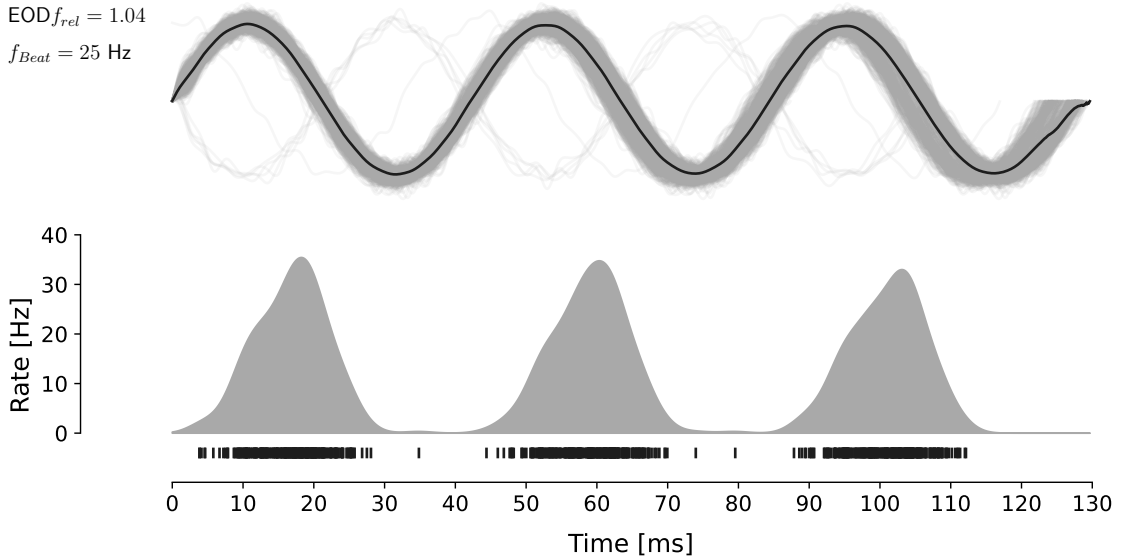


Figure 7 | Beat coupling. **Top:** The stimulus over time with a relative $EODf$ of 1,04 and a beat frequency of 25 Hz ($n=5187$). **Bottom:** Spike rate estimated with a Gaussian kernel with spike raster of all trials plotted in one.

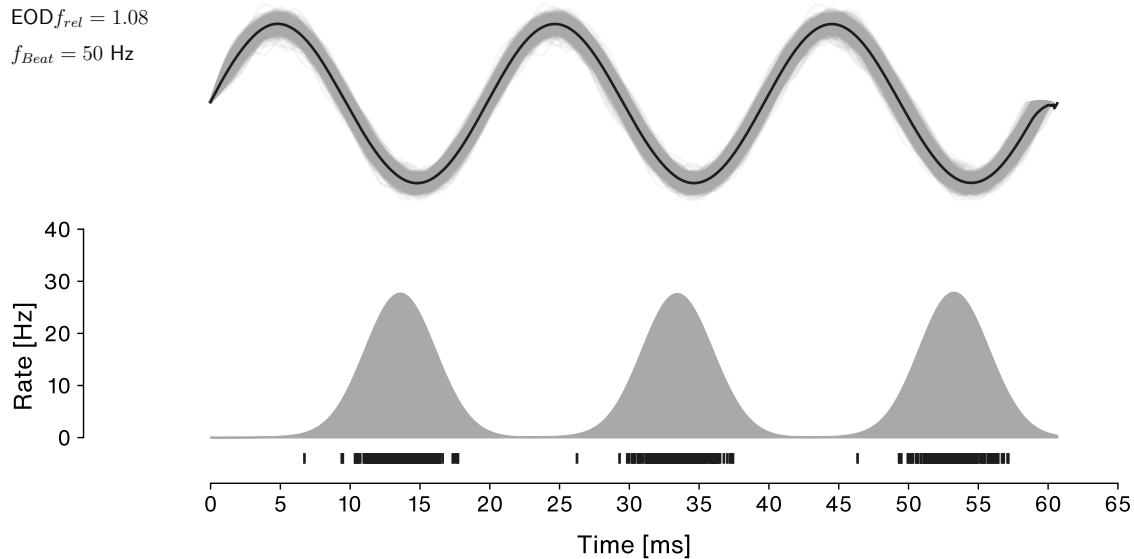


Figure 8 | Beat coupling. **Top:** The stimulus over time with a relative EOD f of 1,08 and a beat frequency of 50 Hz (n=2427). **Bottom:** Spike rate estimated with a Gaussian kernel with spike raster of all trials plotted in one.

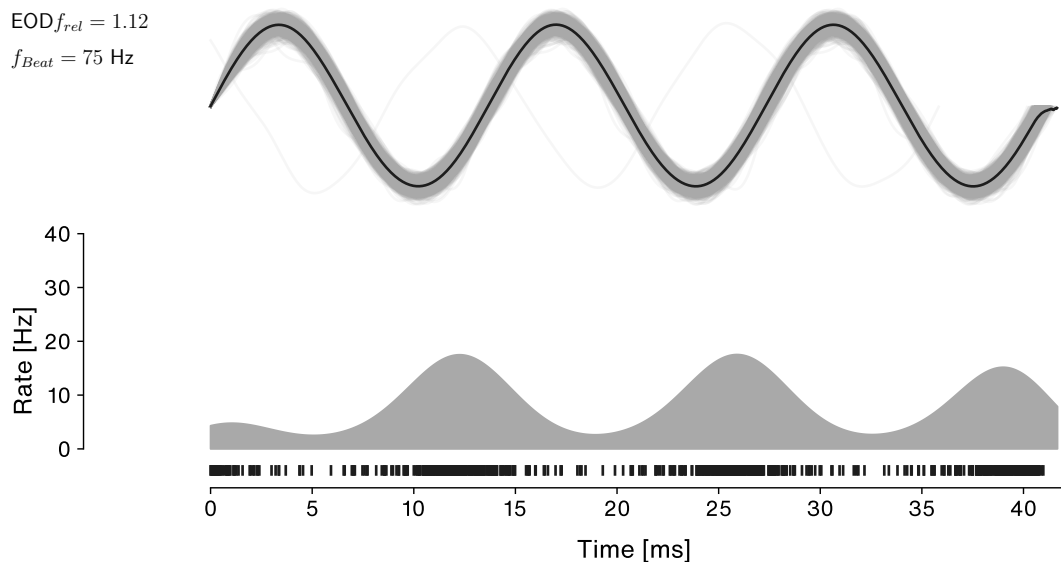


Figure 9 | Beat coupling. **Top:** The stimulus over time with a relative EOD f of 1,12 and a beat frequency of 75 Hz (n=1667). **Bottom:** Spike rate estimated with a Gaussian kernel with spike raster of all trials plotted in one.

To confirm our suspicion that this cell was encoding troughs, we analyzed the responses to a stimulus with a step-wise decreasing and increasing amplitude. The response of the cell to this stimulus confirmed our suspicion that the cell was conveying information about troughs in amplitude. If the amplitude had a negative contrast (meaning -30 % under the amplitude of the EOD of the fish), the firing rate was high with around 10 Hz to 15 Hz and with positive contrast, the firing rate declined to 3 Hz to 5 Hz (Figure 10).

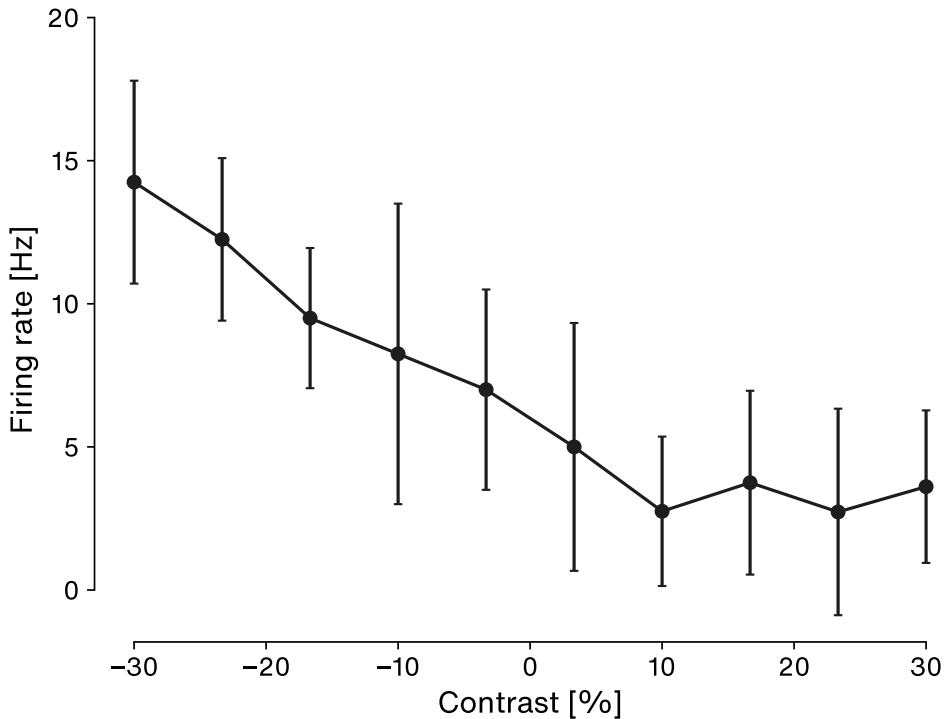


Figure 10 | Frequency-current curve. The FI-curve of the neuron we recorded shows an elevated firing rate to strongly negative contrasts, which decreases as the contrast increases and stays at a constantly low firing rate for all contrasts above 10% (n=10 for every data point, [mean \pm std])

To see how fast our cell is responding to our stimulus we estimated the spike triggered average (STA). The STA had a trough around -10 ms before the centered spikes which occurred at the time zero. To put this into perspective the duration of -10 ms is the time between registration of the stimulus to the response of the cell. The negative peak of the curve was also further confirming our suspicion, that the cell was responding to troughs in the stimulus (Figure 11).

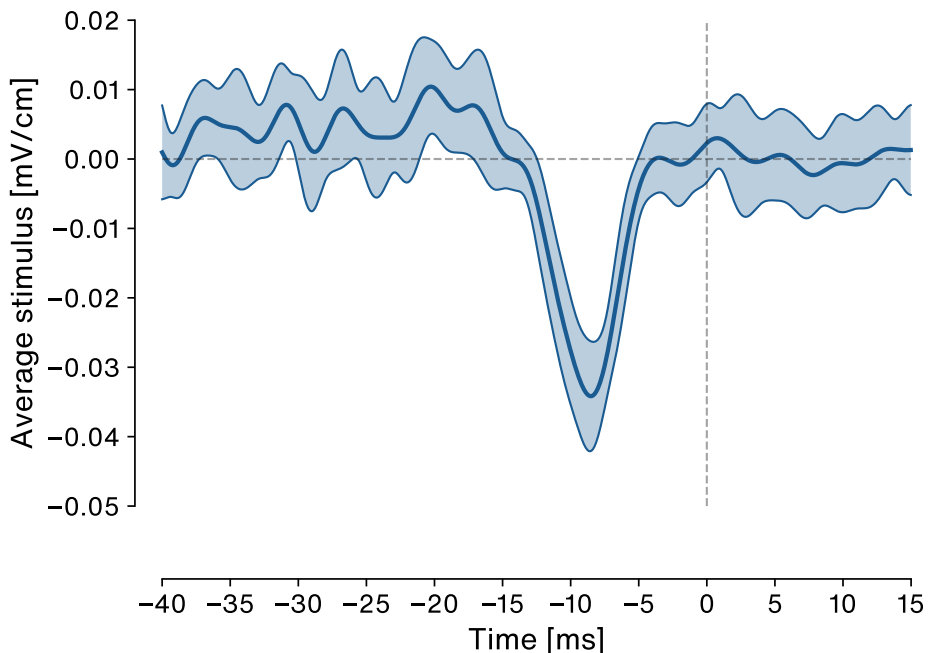


Figure 11 | Spike triggered average (STA). Average stimulus [mV cm^{-1}] over at time zero centered spikes. The stimulus was random amplitude modulation (RAM) for 3,82 min.

To summarise this section, we found out that our principal cell was not coding for communication signals (chirps), but had an increased firing rate if the stimulus amplitude declined. These results indicate that our principal cell is a superficial OFF-cell. On this finding, we based the following analysis and focused on the bursting behavior.

3.2 Bursting behavior and stimulus reconstruction

During our analyses of the neuron's baseline activity, we discovered that the neuron we worked with showed a firing pattern that included distinct bursts and single spikes. We developed a simple algorithm that groups spikes that are less than 10 ms apart as bursts. We considered these bursts as single events in time that occurred at the time of the first spike inside a burst. Since our neuron responded to beats at mainly negative contrast levels, we wanted to quantify to which degree single spikes and bursts contribute to the information the neuron encodes (Figure 12).

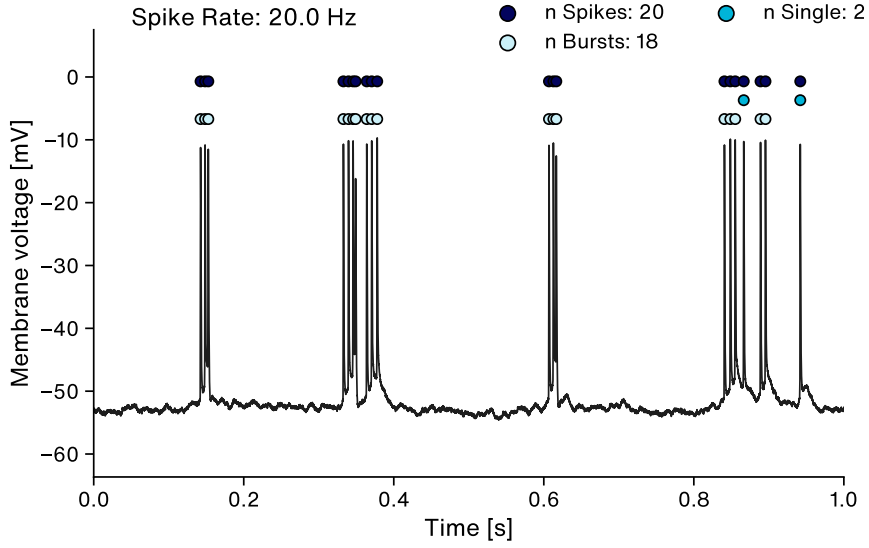


Figure 12 | Bursty baseline activity. Our baseline recordings already showed that the neuron of interest tended to either produce single, sparse spikes or bursts, in which multiple spikes occur in rapid succession.

We used random amplitude modulations (RAM) to stimulate the fish. We then used the envelope of the resulting beat, i.e. the RAM superimposed onto the fish's own EOD f and computed the average stimulus that elicited a spike. To quantify the information encoded in spikes and bursts separately, we computed the spike-triggered average (STA) stimuli for both events and reconstructed the stimulus by convolving the STA with the respective time series. The STA from single spikes closely resembles the overall STA (Figure 13 A, Figure 11). The STA for the bursts exhibits a noisier shape (Figure 13 B, Figure 11). This pattern is consequently reflected in the stimulus reconstruction: The reconstructed stimulus closely follows the troughs of the original stimulus. Only troughs can be reconstructed, since the STA resembles a trough. The reconstructions for the original spike train and the extracted single spikes are almost identical. For the extracted bursts the reconstructions are noisier and does not follow the original stimulus as well Figure 14.

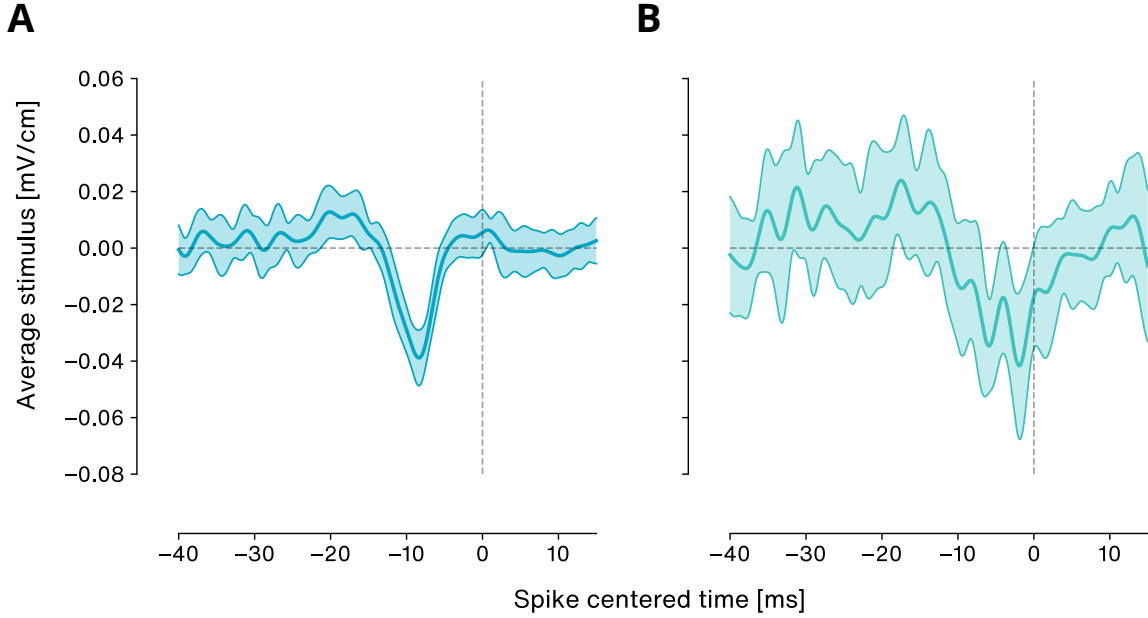


Figure 13 | Spike- and burst triggered average stimulus. The STA for single spikes (A) resembles a clear trough, similar to the overall STA. The STA for the extracted burst is also a trough but the profile is much noisier.

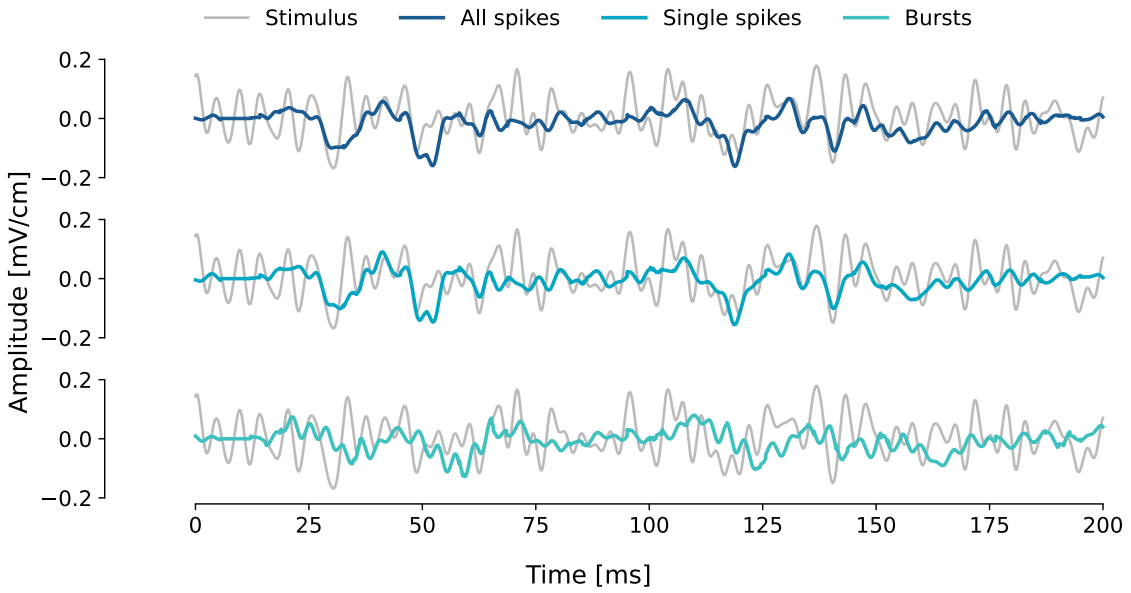


Figure 14 | Stimulus reconstruction. Reconstructed stimulus using the three STAs as kernels. The original stimulus is indicated as the light gray bar behind the colored reconstructions.

To quantify the difference between the original and the reconstructed stimuli, we computed, and compared, the euclidean distance between stimulus and the reconstructed reconstructed stimulus via the triggered averages of single spikes and bursts (Figure 15). We found that the euclidean distance for single chirps and all chirps combined had approximately the same median, whereas the median of the euclidean distance for bursts was strongly elevated. This indicates, that bursts, if considered separately, are not sufficient to encode the stimulus.

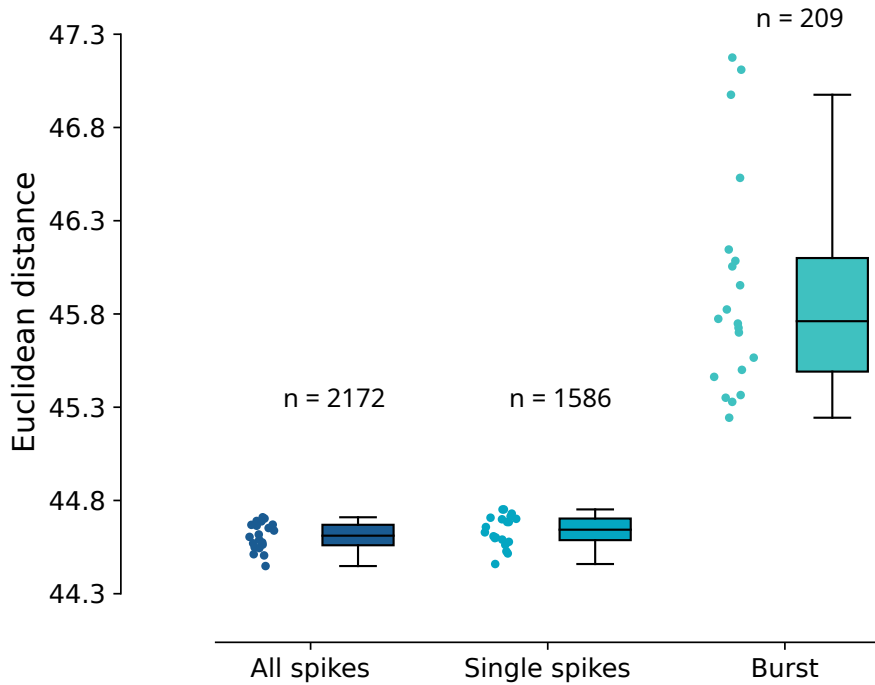


Figure 15 | Comparison between reconstructed- and original stimuli for all spikes, single spikes and bursts respectively. The median euclidean distance does not differ strongly between the original spike-train and all single spikes. The mean euclidean distance for bursts is strongly elevated compared to the other two categories.

4 Discussion

The principal cell we recorded from the ELL didn't convey information to a stimulus mimicking a conspecific which is emitting chirps (communication signals). Furthermore, we showed that the cell was coupled with the stimulus beat, without any chirps in it. The firing rate of the cell in response to the beat was higher if there was a trough and lower if there was a peak in the beat stimulus. This indicates that the principal cell was a superficial OFF-cell. The stimulus reconstruction of this cell further confirms our hypothesis that we found a superficial OFF-cell, displaying a trough 10 ms before a spike occurs. Dividing the spikes used for the stimulus reconstruction into different classes, all spikes, bursting spikes and single spikes, displayed that bursting spikes (ISIs < 10 ms) did worse in the reconstruction than the other classes.

4.1 The principal cell was not responding to chirps

As already seen and mentioned our principal cell did not respond to chirps in a global manner. We could see in one trial an OFF response of the cell, but this was only found with specific settings ($EODf$: 1.05, f_{Beat} : 30 Hz). The recorded cell was not encoding chirps which can be explained by the importance to differentiate at which phase of the stimulus beat the chirp is occurring. Metzen et al., 2016 displayed for an OFF-cell in the ELL that if the chirp is occurring at a beat phase of zero to π the firing rate is decreased whereas at a phase for π to 2π the firing rate was increased. We only worked from a global perspective and pooled our results together, meaning we pooled chirp occurrences in all beat phases, which makes the chirp response a flat line. On the other hand, OFF-cells filter the signal with a low-pass filter, so responses to a high-frequency excursion could not be clearly visible (Marsat et al., 2009).

4.2 The principal cell was a superficial OFF-cell

We could see a classical OFF response to the simulation of a non-chirping conspecific. The firing rate increased from 0 Hz to 30 Hz while the beat amplitude was decreasing. This response behavior was further explored/classified with an F-I curve and an STA, both validating the hypothesis that our principal cell was a superficial OFF-cell. The increase in firing rate for negative contrasts in the F-I curve and the trough before a spike occurs in the STA are clear signs that this cell is responding to decreasing beat amplitudes. The trough in the STA was near the 10 ms mark which is indicating the delay period for the cell to respond to our stimulus. This could be observed with higher beat frequencies, where the response was weaker and shifted in the beat phase. One part of the delay period is determined by the time constant of the cell: If the stimulus frequency is pushed beyond a certain cutoff frequency, the phase of the response shifts and lags behind the stimulus, until the response deteriorates completely. The other part is that it takes time for the signal to get from our stimulating electrodes, and then from the sensory cell over the P-units to the cells in the ELL.

4.3 Bursting is not sufficient for stimulus reconstruction

The grouping from interspike intervals to bursting and single spikes was done by setting a threshold at 10 ms. This threshold was fine for our baseline recordings, but as for the RAM stimulus, we didn't detect many bursts, which is one of the major differences between the burst and single spike classes. This abundance of bursts is making the STA noisy and the spread in the euclidean distance high, meaning that the explanatory value for what bursting behavior is used for is very low. Marsat et al., 2009 could show that bursts in the CMS and CLS could be detected if the amplitude modulation of the beat changed by a local low frequency (prey mimics). The low count of bursts for the RAM stimulus could be also identified

by Marsat et al., 2009, where they found out that the ISIs (interspike intervals) are longer compared to the other ELL regions (CMS and CLS). This analysis by Marsat et al., 2009 was done in ON-cells, but for our OFF-cell, we see for this aspect no differences. Bursting behavior in pyramidal ELL cells can act as feature detectors for fast-changing amplitude modulations. This was displayed by Gabbiani et al., 1996 for ON and OFF cells in the ELL. In comparison to our OFF-cell we didn't see, for fast-changing stimuli, an increase in bursting behavior.

Another factor is that bursts of pyramidal cells in the ELL encode for chirps (Marsat et al., 2009) and because we couldn't see any responses from our OFF-cell, we didn't analyze bursting behavior while simulating chirps. This analysis could be useful for future reference.

4.4 Summary

For our project, we recorded cells in the ELL specifically in the LS. We found one principal OFF-cell, which didn't respond to a simulated chirping conspecific. The OFF cell was characterized by a high firing rate for negative contrast levels and a trough in the STA 10 ms before the spike occurs. The stimulus reconstruction was then further divided into burst (ISIs < 10 ms) and single spikes, which yielded mixed results. The reconstruction for bursts was mostly noisy and not good for fast-changing stimuli. The main factor was the low count of bursts detected.

Literature

- Ackermann, Hermann et al. (2014). "Brain mechanisms of acoustic communication in humans and non-human primates: An evolutionary perspective". In: *Behavioral and Brain Sciences* 37.6, pp. 529–546. doi: 10.1017/S0140525X13003099.
- Adrian, Stoewer et al. (2014). "File format and library for neuroscience data and metadata". In: *Frontiers in Neuroinformatics* 8.
- Bastian, Joseph et al. (1991). "Morphological correlates of pyramidal cell adaptation rate in the electrosensory lateral line lobe of weakly electric fish". In: *Journal of Comparative Physiology A* 168.4, pp. 393–407.
- Berman, Neil J. et al. (1998). "Inhibition Evoked From Primary Afferents in the Electrosensory Lateral Line Lobe of the Weakly Electric Fish (*Apteronotus leptorhynchus*)". In: *Journal of Neurophysiology* 80.6. PMID: 9862915, pp. 3173–3196. doi: 10.1152/jn.1998.80.6.3173.
- Carr, Catherine E. et al. (1982). "Peripheral organization and central projections of the electrosensory nerves in gymnotiform fish". In: *Journal of Comparative Neurology* 211.2, pp. 139–153. doi: <https://doi.org/10.1002/cne.902110204>.
- Catania, Kenneth C (2015). "Electric eels use high-voltage to track fast-moving prey". In: *Nature communications* 6.1, pp. 1–6.
- Engler, G et al. (2000). "Spontaneous modulations of the electric organ discharge in the weakly electric fish, *Apteronotus leptorhynchus*: a biophysical and behavioral analysis". In: *Journal of Comparative Physiology A* 186.7, pp. 645–660.
- Gabbiani, Fabrizio et al. (1996). "From stimulus encoding to feature extraction in weakly electric fish". In: *Nature* 384.6609, pp. 564–567.
- Hagedorn, Mary et al. (1985). "Court and spark: electric signals in the courtship and mating of gymnotoid fish". In: *Animal Behaviour* 33.1, pp. 254–265. ISSN: 0003-3472. doi: [https://doi.org/10.1016/S0003-3472\(85\)80139-1](https://doi.org/10.1016/S0003-3472(85)80139-1).
- Harris, Charles R. et al. (Sept. 2020). "Array programming with NumPy". In: *Nature* 585.7825, pp. 357–362. doi: 10.1038/s41586-020-2649-2.
- Heiligenberg, Walter et al. (1982). "Labelling of electroreceptive afferents in a gymnotoid fish by intracellular injection of HRP: The mystery of multiple maps". In: *Journal of comparative physiology* 148.3, pp. 287–296.
- Hunter, J. D. (2007). "Matplotlib: A 2D graphics environment". In: *Computing in Science & Engineering* 9.3, pp. 90–95. doi: 10.1109/MCSE.2007.55.
- Hupé, Ginette J. et al. (May 2008). "Electrocommunication signals in free swimming brown ghost knifefish, *Apteronotus leptorhynchus*". In: *Journal of Experimental Biology* 211.10, pp. 1657–1667. ISSN: 0022-0949. doi: 10.1242/jeb.013516.
- Kalmijn, A. J. (Oct. 1971). "The Electric Sense of Sharks and Rays". In: *Journal of Experimental Biology* 55.2, pp. 371–383. ISSN: 0022-0949. doi: 10.1242/jeb.55.2.371.

- Kanwal, Jagmeet S. (2018). "Chapter 46 - Ultrasonic Social Communication in Bats: Signal Complexity and Its Neural Management". In: *Handbook of Ultrasonic Vocalization*. Ed. by Stefan M. Brudzynski. Vol. 25. Handbook of Behavioral Neuroscience. Elsevier, pp. 493–508. doi: <https://doi.org/10.1016/B978-0-12-809600-0.00046-9>.
- Marsat, Gary et al. (2009). "Transient Signals Trigger Synchronous Bursts in an Identified Population of Neurons". In: *Journal of Neurophysiology* 102.2, pp. 714–723. doi: 10.1152/jn.91366.2008.
- Metzen, Michael G et al. (Apr. 29, 2016). "Neural Correlations Enable Invariant Coding and Perception of Natural Stimuli in Weakly Electric Fish". In: *eLife* 5, e12993. issn: 2050-084X. doi: 10.7554/eLife.12993.
- Metzner, W et al. (1997). "A sensory brain map for each behavior?" In: *Proceedings of the National Academy of Sciences* 94.26, pp. 14798–14803.
- (1997). "A sensory brain map for each behavior?" In: *Proceedings of the National Academy of Sciences* 94.26, pp. 14798–14803. doi: 10.1073/pnas.94.26.14798.
- Nelson, M. E. et al. (Oct. 1, 1997). "Characterization and modeling of P-type electrosensory afferent responses to amplitude modulations in a wave-type electric fish". In: *Journal of Comparative Physiology A* 181.5, pp. 532–544.
- Raab, Till et al. (Oct. 2021). "Electrocommunication signals indicate motivation to compete during dyadic interactions of an electric fish". In: *Journal of Experimental Biology* 224.19. jeb242905. issn: 0022-0949. doi: 10.1242/jeb.242905.
- Rose, Gary J. (2004). "Insights into neural mechanisms and evolution of behaviour from electric fish". In: *Nature Reviews Neuroscience* 5.12, pp. 943–951.
- Seffer, Dominik et al. (2014). "Pro-social ultrasonic communication in rats: Insights from playback studies". In: *Journal of Neuroscience Methods* 234. Measuring Behavior, pp. 73–81. issn: 0165-0270. doi: <https://doi.org/10.1016/j.jneumeth.2014.01.023>.
- team, The pandas development (Feb. 2020). *pandas-dev/pandas: Pandas*. Version latest. doi: 10.5281/zenodo.3509134.
- Virant-Doberlet, Meta et al. (2004). "Vibrational communication in insects". In: *Neotropical Entomology* 33, pp. 121–134.
- Virtanen, Pauli et al. (2020). "SciPy 1.0: Fundamental Algorithms for Scientific Computing in Python". In: *Nature Methods* 17, pp. 261–272. doi: 10.1038/s41592-019-0686-2.
- Walz, Henriette et al. (2013). "The neuroethology of electrocommunication: How signal background influences sensory encoding and behaviour in *Apteronotus leptorhynchus*". In: *Journal of Physiology-Paris* 107.1. Neuroethology, pp. 13–25. issn: 0928-4257. doi: <https://doi.org/10.1016/j.jphysparis.2012.07.001>.
- Zakon, H. (1986). "The emergence of tuning in newly generated tuberous electroreceptors". In: *Journal of Neuroscience* 6.11, pp. 3297–3308. issn: 0270-6474. doi: 10.1523/JNEUROSCI.06-11-03297.1986.
- Zakon, Harold et al. (2002). "EOD modulations of brown ghost electric fish: JARs, chirps, rises, and dips". In: *Journal of Physiology-Paris* 96.5, pp. 451–458. issn: 0928-4257. doi: [https://doi.org/10.1016/S0928-4257\(03\)00012-3](https://doi.org/10.1016/S0928-4257(03)00012-3).